Screening novel format antibodies to design bispecific ADCs that address target heterogeneity

AACR Annual Meeting 2024
Abstract #2052

Stuart D. Barnscher, Dunja Urosev, Kevin Yin, Andrea Hernandez Rojas, Sam Lawn, Vincent Fung, Jodi Wong, Araba Sagoe-Wagner, Lemlem Degefie, Ali Livernois, Catrina Kim, Paul A. Moore, Jamie R. Rich

Author Affiliations: Zymeworks Inc., Vancouver, BC, Canada

Introduction

Inter-patient and intra-tumoral target heterogeneity is a challenge in the design of antibody-drug conjugates (ADCs) that target a single tumor associated antigen (TAA). Bispecific ADCs that can target two different TAAs both simultaneously and independently may overcome challenges associated with target heterogeneity and the reliance on target co-expression associated with bivalent bispecific antibodies.

Here we describe a novel approach to the design and screening of a FRα x NaPi2b bispecific ADC library with the aim of targeting tumors that express either FRα, NaPi2b, or both targets.

Azymetric™ enables a variety of bispecific formats

- Enables screening of antibodies with different valency, geometry, and affinity
- Desirable drug-like features of IgG-based antibodies
- Compatible with standard manufacturing processes

1+1 Bispecific Format		
2+1 Bispecific Format		
2+2 Bispecific Format		

Figure 1. Table of 11 different bispecific antibody formats across three different target valencies enabled by the Azymetric™ platform. Ven diagrams of the hypothetical co-expression of two targets within a given indication and the potential addressable patient population for the three different formats: a 1+1 bispecific format that contains one binding arm to each target, a 2+1 bispecific format that contains two binding arms to one target and one binding arm to a different target, and a 2+2 bispecific format that contains two binding arms to each target.

Target heterogeneity in patient population

A

B Expression of FRα and NaPi2b in 98 HGSOC samples

NaPi2b \ FRα IHC Score	0	1+	2+	3+
3+	0	1	3	12
2+	1	4	10	26
1+	1	3	4	17
0	2	0	2	12

Figure 2. (A) A hypothetical distribution of patients that express target A, target B, both targets, or neither target. **(B)** Immunohistochemistry score of FRα and NaPi2b in 98 high-grade serous ovarian cancer (HGSOC) patient samples.

Target heterogeneity in tumor mass

A

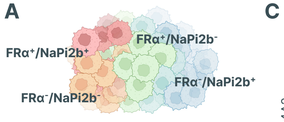

B FRα IHC NaPi2b IHC

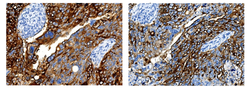

C SLC34A2 and FOLR1 expression within individual patient tumor

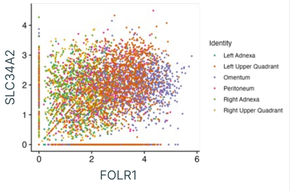

Figure 3. (A) Cartoon of a tumor mass with cells expressing FRα, NaPi2b, both antigens, or neither antigen. **(B)** Immunohistochemistry staining of FRα and NaPi2b from the same patient sample and same region. **(C)** Single cell RNA analysis of treatment-naive high-grade serous ovarian cancer (HGSOC) patient tumor samples.[1]

Paratopes used in bispecific formats

Paratope	Target	FSA cell binding EC_{50} (nM)	OAA cell binding EC_{50} (nM)
12A10	NaPi2b[a]	0.7	3.4
10L18	FRα[b]	0.2	8.5
76	FRα[b]	2.9	3.3
2L16	FRα[b]	0.6	5.8

[a]TOV21G cell line; [b]JEG-3 cell line

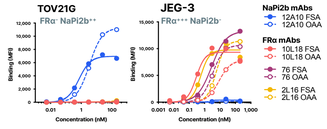

Figure 4. Table and figure of the 4 paratopes used to generate the 48 bispecific antibodies depicting their on-cell binding EC50 for FSA (full sized antibody) and OAA (one armed antibody) on TOV21G and JEG-3 cells. FSA: full sized antibody; OAA: one armed antibody.

Generation and analytical characterization of 48 bispecific antibodies

Bispecific format	Bispecific ID	Chain A paratope	Chain B paratope	Monomer (%)	Reoxidized Bispecific (%)	Expected Mass (Da)	Expected mass detected	Mass signal (%)
1+1 Bispecific Format	Bsp1	12A10	10L18	94	93	145,226	Yes	80
	Bsp2	12A10	76	95	91	146,624	Yes	100
	Bsp3	12A10	2L16	94	92	145,950	Yes	92
2+1 Bispecific Format, N-term	Bsp4	12A10	2 x 10L18	94	97	193,059	Yes	100
	Bsp5	12A10	2 x 76	93	96	195,874	Yes	100
	Bsp6	12A10	2 x 2L16	92	93	194,512	Yes	100
	Bsp7	10L18	2 x 12A10	96	95	193,537	Yes	100
	Bsp8	76	2 x 12A10	95	95	194,936	Yes	100
	Bsp9	2L16	2 x 12A10	94	95	194,264	Yes	100
2+1 Bispecific Format, C-term	Bsp10	12A10	2 x 10L18	94	95	193,055	Yes	100
	Bsp11	12A10	2 x 76	94	93	195,875	Yes	100
	Bsp12	12A10	2 x 2L16	94	94	194,512	Yes	100
	Bsp13	10L18	2 x 12A10	94	7	193,612	Yes	38
	Bsp14	76	2 x 12A10	95	4	195,017	Yes	34
	Bsp15	2L16	2 x 12A10	93	4	194,338	Yes	40
2+2 Bispecific Format, N-term	Bsp16	2 x 12A10	2 x 10L18	92	91	241,372	Yes	86
	Bsp17	2 x 12A10	2 x 76	93	97	244,189	Yes	89
	Bsp18	2 x 12A10	2 x 2L16	89	89	242,826	Yes	84
2+2 Bispecific Format, C-term	Bsp19	2 x 12A10	2 x 10L18	95	3	241,445	Yes	71
	Bsp20	2 x 12A10	2 x 76	96	2	244,279	Yes	83
	Bsp21	2 x 12A10	2 x 2L16	94	4	242,909	Yes	91
1+1	Bsp22	76 scFv	12A10	91	51	124,837	Yes	100
	Bsp23	2L16 scFv	12A10	94	47	125,564	Yes	100
2+1 Bispecific Format, N-term	Bsp24	2 x 2L16	12A10	93	31	172,877	Yes	100
	Bsp25	2 x 12A10	10L18	95	2	172,035	Yes	85
	Bsp26	2 x 12A10	76	95	2	173,436	Yes	100
	Bsp27	2 x 12A10	2L16	94	3	172,762	Yes	77
	Bsp28	12A10 Fab + 76 scFv	76	86	32	173,922	Yes	100
	Bsp29	12A10 Fab + 2L16 scFv	2L16	95	36	172,891	Yes	100
2+1 Bispecific Format, C-term	Bsp30	2 x 10L18	12A10	94	27	171,566	Yes	100
	Bsp31	2 x 76	12A10	84	31	174,069	Yes	100
	Bsp32	2 x 2L16	12A10	90	33	173,020	Yes	100
	Bsp33	2 x 12A10	10L18	95	2	172,178	Yes	77
	Bsp34	2 x 12A10	76	95	2	173,577	Yes	54
	Bsp35	2 x 12A10	2L16	94	2	172,900	Yes	72
2+2 Bispecific Format, N-term	Bsp36	2 x 2L16	2 x 12A10	96	17	221,190	Yes	100
	Bsp37	2 x 12A10	2 x 10L18	94	1	219,868	Yes	76
	Bsp38	2 x 12A10	2 x 76	94	5	222,579	No	0
	Bsp39	2 x 12A10	2 x 2L16	91	4	221,201	No	0
2+2 Bispecific Format, C-term	Bsp40	2 x 10L18	2 x 12A10	94	0	219,888	No	0
	Bsp41	2 x 76	2 x 12A10	85	4	222,511	Yes	67
	Bsp42	2 x 2L16	2 x 12A10	91	1	221,345	No	0
	Bsp43	2 x 12A10	2 x 10L18	93	1	220,037	Yes	82
	Bsp44	2 x 12A10	2 x 76	94	1	222,837	Yes	100
	Bsp45	2 x 12A10	2 x 2L16	87	4	221,510	Yes	90
2+2 Bispecific Format, N+C-term	Bsp46	2 x 12A10 + 10L18 scFv	10L18	95	15	219,758	Yes	100
	Bsp47	2 x 12A10+ 76 scFv	76	89	14	222,248	Yes	100
	Bsp48	2 x 12A10 + 2L16 scFv	2L16	95	13	221,209	Yes	100

Figure 5. Table of 48 bispecific antibodies and their analytical characterization. Monomer content was assessed by high performance liquid chromatography size exclusion chromatography (HPLC-SEC). The monomer peak of each bispecific antibody was identified as the peak with the same retention time as monospecific control antibodies. Reoxidation was assessed by capillary electrophoresis sodium dodecyl-sulfate (CE-SDS). Reoxidized antibodies were identified by bands of the corresponding size on non-reducing CE-SDS and the extent of reoxidation determined by the band density relative to other expected antibody fragments. Intact liquid chromatography mass spectroscopy (LC-MS) was used to confirm the identity of the bispecific antibody and to determine the presence of homodimers. The expected mass was calculated using the primary sequences of each half antibody component in addition to expected post-translation modifications. The mass signal was calculated as a percentage of the signal intensity of the desired heterodimer over the total signal intensity of heterodimer and homodimer species.

In vitro functional characterization of 48 bispecific antibodies and ADCs

A

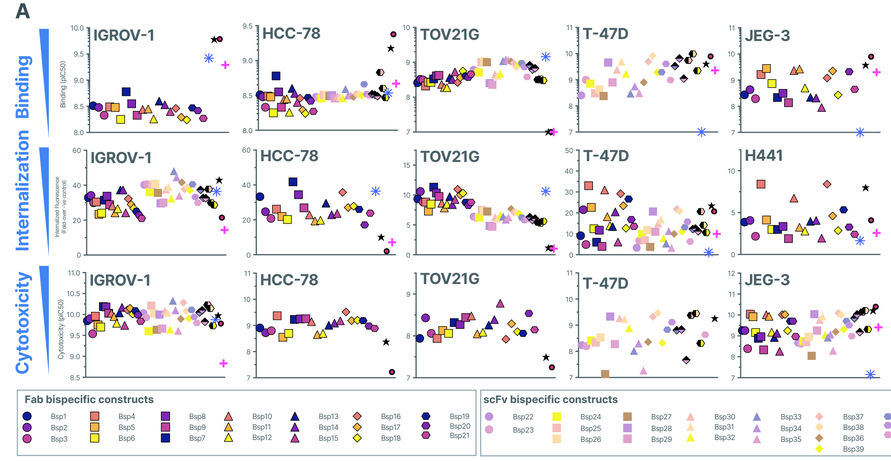

B

Cell line	FRα/cell	NaPi2b/cell	FRα/NaPi2b
EBC-1 (NSCLC)	0	0	- / -
TOV21G (OC)	6,000	350,000	- / ++
H1781 (NSCLC)	15,000	250,000	+ / ++
H441 (NSCLC)	190,000	41,000	++ / +
H2110 (NSCLC)	430,000	70,000	++ / +
HCC-78 (NSCLC)	500,000	800,000	+++ / +++
T-47D (BC)	550,000	6,000	+++ / -
JEG-3 (PCC)	1,200,000	11,000	+++ / -
IGROV-1 (OC)	2,900,000	1,600,000	++++ / +++

C Modest differences in binding to cells that co-express both targets

D Fab and scFv 1+1, 2+1 and 2+2 formats showed similar trends in cytotoxicity in target co-expressing cell line models

E FRα paratope-based differences in potency

F Identification of high potency Fab and scFv bispecific ADCs

Figure 6. (A) Binding affinities (pIC_{50}), internalization (internalized fluorescence fold-over negative IgG1 control values), and cytotoxicity (pIC_{50}) summary for 48 bispecific antibodies and ADCs. Binding and internalization to endogenous expressing cancer cell lines was assessed by flow cytometry, following 24-hour incubation with bispecific mAbs. Cytotoxicity was assessed following a 4-day incubation with bispecific ADCs prior to cell viability assesment. Monospecific NaPi2b and FRα-targeting mAb and ADC controls are shown as available. **(B)** Nine cancer cell line panel, NaPi2b/cell and FRα/cell quantification performed by flow cytometry using AF647-labelled NaPi2b and FRα-targeting mAbs. **(C)** Representative cell binding dose-response curves for 21 Fab and 27 scFv bispecific constructs. **(D, E)** Representative cytotoxicity dose-response curves for 21 Fab and 27 scFv bispecific ZymeLink™ auristatin ADCs in a panel of nine cancer cell lines. **(F)** cytotoxicity (pIC_{50}) vs. cellular internalization (fold-over control) correlation plots in the same cancer cell line or different cell line pairs, blue boxes highlight interesting FRαxNaPi2b bispecific paratope combinations.

Bispecific antibody and ADC generation and characterization workflow

Figure 7. Schematic of the workflow used to generate 48 bispecific antibodies and their corresponding ZymeLink™ Auristatin ADCs. The desired corresponding half-antibody components were reduced in a single pot. Following removal of reducing agent, each reaction was split in half with one portion undergoing oxidation and the other undergoing conjugation. Biophysical and cell-based assays were performed using high throughput methods for both mAbs and ADCs.

Conclusions

- 48 bispecific antibodies and ADCs were generated using an Azymetric™ workflow employing 4 different paratopes and 11 formats.
- Bispecific formats containing the 10L18 FRα paratope were more active compared to formats containing 76 or 2L16 FRα paratopes.
- Formats with two 12A10 NaPi2b paratopes were more active.
- 2+2 and 2+1 bispecific formats were more active in a broader range of cell lines compared to 1+1 bispecific formats.
- 2+2 N-term Fab bispecific formats were more cytotoxic than 2+2 C-term Fab formats.
- Similar functional trends were observed for similar formats across Fab-only and scFv-containing bispecifics.

References
1) Vazquez-Garcia et al 2022 Nature 612: 778